Journal of Chromatography A, 1237 (2012) 86–95

Contents lists available at SciVerse ScienceDirect

Journal of Chromatography A

journal homepage: www.elsevier.com/locate/chroma

Optimizing a chromatographic three component separation: A comparison of mechanistic and empiric modeling approaches☆

A. Osberghaus[a], S. Hepbildikler[b], S. Nath[b], M. Haindl[b], E. von Lieres[c], J. Hubbuch[a,*]

[a] Institute of Process Engineering in Life Sciences, Section IV: Biomolecular Separation Engineering, Karlsruhe Institute of Technology, Engler-Bunte-Ring 1, 76131 Karlsruhe, Germany
[b] Pharmaceutical Biotech Production, Roche Diagnostics GmbH, Nonnenwald 2, 82377 Penzberg, Germany
[c] Institute of Bio- and Geosciences 1, Research Center Jülich, 52425 Jülich, Germany

ARTICLE INFO

Article history:
Received 31 October 2011
Received in revised form 29 February 2012
Accepted 9 March 2012
Available online 16 March 2012

Keywords:
Ion exchange chromatography
Design of experiments
Response surface modeling
Mechanistic modeling
Steric mass action (SMA)
Separation optimization

ABSTRACT

The search for a favorable and robust operating point of a separation process represents a complex multi-factor optimization problem. This problem is typically tackled by design of experiments (DoE) in the factor space and empiric response surface modeling (RSM); however, separation optimizations based on mechanistic modeling are on the rise. In this paper, a DoE–RSM-approach and a mechanistic modeling approach are compared with respect to their performance and predictive power by means of a case study – the optimization of a multicomponent separation of proteins in an ion exchange chromatography step with a nonlinear gradient (ribonuclease A, cytochrome *c* and lysozyme on SP Sepharose FF). The results revealed that at least for complex problems with low robustness, the performance of the DoE-approach is significantly inferior to the performance of the mechanistic model. While some influential factors of the system could be detected with the DoE–RSM-approach, predictions concerning the peak resolutions were mostly inaccurate and the optimization failed. The predictions of the mechanistic model for separation results were very accurate. Influences of the experimental factors could be quantified and the separation was optimized with respect to several objectives. However, the discussion of advantages and disadvantages of empiric and mechanistic modeling generates synergies of both methods and leads to a new optimization concept, which is promising with respect to an efficient employment of high throughput screening data.

1. Introduction

Ion exchange chromatography (IEC) is a widely used application in biomolecular downstream processing. In IEC, the main focus is the separation of a target component from a protein mixture – preferably in a step elution, but complex separation problems may require linear or even nonlinear gradient elutions. In addition to the shape of the elution gradient, the quality of a separation depends on several process factors, among others the employed buffers and salts. Furthermore, the objectives of a separation step are not only defined by high yields and product purity, but also by additional demands, such as process robustness, financial and ecological constraints. Thus, the optimization of a separation step is a multiparametric and multiobjective problem.

The approaches to tackle problems of this kind are various and can be roughly divided into search algorithms and modeling methods. Various successful applications of search algorithms for separation optimization have been published during the last 30 years. The application of simplex algorithms, for example, has been proved successful for example in [1–3]. Recently, more robust search algorithms like neural network approaches (see in [4–6]), simulated annealing (for example in [7]) and evolutionary algorithms (see [8,9]) have been successfully applied to optimization in chromatography. While the low mathematical effort of search methods and their high performance in noisy systems was demonstrated in these research publications, a critical drawback of search methods is given by the tremendous experimental effort and the low knowledge gain about the examined system, particularly about sensitivity and robustness aspects.

However, the importance of process understanding, as well as robustness and sensitivity analyses was only recently emphasized in guidelines, published by the US Food and Drug Administration [10]. Consequently, multivariate optimization approaches based on design of experiments (DoE) and empiric response surface modeling (RSM) are increasingly applied in bioseparation process development, because they allow for the characterization of design factor spaces and for the calculation of optimal system settings and their robustness. Similar to the application of search algorithms,

☆ I kindly thank Marie-Luise Schwab, who performed some of the experimental work referred to in this publication.
* Corresponding author. Tel.: +49 721 608 42557; fax: +49 721 608 46240.
E-mail address: juergen.hubbuch@kit.edu (J. Hubbuch).

0021-9673/$ – see front matter © 2012 Elsevier B.V. All rights reserved.
doi:10.1016/j.chroma.2012.03.029

first publications on the application of DoE–RSM in the field of ion exchange chromatography have been published in the eighties, for example by [11] who optimized a separation step in reversed-phase chromatography based on a full-factorial design. DoE–RSM techniques were successfully applied and further developed in chromatography studies, for example in [12] (full factorial design), [13] (block design and partial least squares-regression) and [14] (fractional factorial design, application of modeling software). Reviews on DoE–RSM methods, like in [15], comparison studies of regression algorithms [16] or the formulation of very specific regression functions like in [17] demonstrate that DoE–RSM is well established in the optimization of IEC steps.

Alternatively to this empiric modeling approach, the application of mechanistic modeling for the optimization of IEC steps is on the rise due to time efficiency of algorithms and increased calculation power (see argumentation lines in [18,19]). Mechanistic modeling means to employ functional relationships between physical parameters in chromatography and retention times or even complete chromatograms. Important reviews on mechanistic modeling are for example [18,20,21] or [22] Successful optimizations based on mechanistic modeling of IEC processes have been demonstrated for step gradients [23], linear gradients [24] and displacement systems [25]. Additionally, a validated model proves to be an accurate prediction tool and lends itself to application in process control, which was demonstrated for example in [26,27]. A drawback of separation optimization based on a mechanistic model seemed to be the very time consuming procedure of repeatedly solving the underlying partial differential equation system. However, recently a very efficient and time-optimized solver was introduced by [28] that allows for model-based optimization in a few minutes. As a result, the optimization based on mechanistic modeling is now competitive to the DoE–RSM approach with respect to time efficiency. This will be the dooropener concerning research on the advantages and benefits of mechanistic modeling, especially compared to the established approaches in chromatography process optimization. As to the authors' knowledge there are no studies, where both approaches are compared based on the same set of data. Too little information is available on the predictivity quality of mechanistic modeling in comparison to the DoE–RSM approach, inside and beyond the design space. Furthermore, to the best of the authors' knowledge, there is only little research on the performance of DoE in separation problems with low robustness.

However, low robustness is very common in separation problems, as slight changes in the level of salt buffers in step or gradient elutions have significant influence on retention times and peak shapes. Considering this, the optimization performance of a model based on mechanistic understanding should exceed the performance of an empiric model. An important aim of the manuscript is to show, if the difference in performance is significant.

Another drawback of the previously cited optimization studies is the fact that they have mostly been limited to a fixed objective for the separation process. However, as shown before, separation issues are normally multiobjective or objectives are changed in the development of a chromatography process. Thus, approaches for optimization should be flexible with respect to changing objectives and should not demand for re-calibration.

In this paper, the DoE–RSM approach and the mechanistic modeling approach are compared with respect to the mentioned issues. After a theoretical comparison of both approaches, they are applied to a case study – the optimization of a multicomponent-separation in an IEC step. As two of the proteins have close isoelectric points (cytochrome *c*: 10.0–10.5, lysozyme: 11.35), a bilinear gradient that is a series of two linear salt elution gradients, was chosen for the separation step in analogy to Refs. [8,26]. Due to the bilinear gradient, this model system is rather complex and demands for robustness analyses. According to a D-optimal onion design, experimental data for optimization was planned and the chromatography runs randomly executed. Based on this randomly derived DoE-planned data, the RSM-approach as well as the approach of mechanistic modeling in IEC were used for determination of the factor effects on the chromatographic result and for optimization. Further, the additional effort for separation optimization with respect to changing objectives was analysed, as well as model predictiveness regarding factor sets beyond the original design space. The application of both modeling approaches to this case study allowed for an improved comparison of performance and effort with respect to multivariate separation issues.

2. Theory

2.1. Response surface modeling and design of experiments

Response surface modeling (RSM) is a statistical technique for the a posteriori analysis of experimental data; a regression function t'stof whatever nature – the response surface model – is fitted to the experimental results. Common applied response surface models in IEC have linear or quadratic complexity and are empiric (not mechanistic). Popular regression models are, for example, multivariate quadratic functions.

Let $x_1, x_2, \ldots, x_n$ be the n selected factors for process description and y_i the response/objective value to a specific factor setting x_{1i}, $x_{2i}, \ldots, x_{ni}$. The regression fit of an n-variate quadratic function to the set of m responses $y_1, \ldots, y_m$, is described by:

$$y_i = a_1 + b_1x_{1i} + b_2x_{2i} + \ldots + b_nx_{ni} + c_1x_{1i}^2 + c_2x_{2_i}^2 + \ldots + c_nx_{ni}^2 + d_{1,2}x_{1i}x_{2i} + d_{1,3}x_{1i}x_{3i} + \ldots + d_{n-1,n}x_{n-1,i}x_{ni} \quad (1)$$

for all $1 \le i \le m$. The parameter a_1 is a constant added to the function (see intercept terms in linear regression); furthermore, the values of the parameters b_k for $1 \le k \le n$ display the magnitude of linear influence of the factors x_k. The values of the parameters c_k with $1 \le k \le n$ quantify quadratic influences of the factors x_k and the mixed effects/interaction terms of two-components are quantified by the parameters d_{12} to $d_{n-1,n}$. A higher than quadratic complexity in the examined system leads to high prediction errors. However, high prediction errors give no hints as to the reasons in detail and no direction how to correct the model.

RSM is often behold as a DoE-technique, which is not correct. On the contrary, if a quadratic surface has to be fitted to the results, a well-selected DoE provides an adequate planning of the experiments. Thus, the idea of 'DoE' summarizes a diversified collection of statistical approaches for the maximization of specific information in experimental planning. The advantage of the DoE–RSM-approach, compared to simple screenings, is the provision of experimental designs with high information contents, quick information on reasonable factor ranges and first evidence of factor effects and system robustness.

Common and frequently used experimental plans are full-factorial designs or fractional–factorial designs. They deliver regular screening patterns over a factor space and provide the information for multilinear quadratic response models. Other designs meet special experimental constraints or a-priori-information on the system. For example, space filling designs are best when there is little or no information about the underlying effects of factors on responses while D-optimal designs guarantee high information in the single experiment by minimizing the covariance of the parameter estimates.

2.2. Theory on mechanistic modeling

A mechanistic model imitates the physical processes that occur in the observed system and describes them based on a set of mathematical equations. Thus, typical rate models for chromatographic processes contain convective and diffusive flows through a compressed pile of particles on the column level and the imitation of mass transfer resistances and surface interactions on particle level. In IEC modeling the transition of components from column to particle level is commonly modeled assuming a film; the sorption of protein on the particle surface can be imitated by the steric-mass-action-(SMA) model, developed by [29] and commonly used for the modeling of salt gradient elutions in IEC, for example in [30–32]. For the solution of the whole differential-algebraic equation system, Danckwerts' boundary conditions were applied [33]. For more details on rate models see [18].

In this case study, the decision concerning the most reasonable model complexity was taken in favor of the lumped transport-dispersive approach. This model, including convective, dispersive processes, mass transfer resistances and the SMA model for sorption kinetics, was solved in MatLab® on a Dual Core Processor with 2.81 GHz in approximately 10 s with a density of 200 knots over the whole column length. That is a time span of reasonable brevity, since the model has to be solved hundreds of times in model-based optimization.

The time- and position-dependent change of concentration on column level for the ith component, $\partial c_i/\partial t$, is described by Eq. (2). The first term on the right hand side of Eq. (2) describes the convective transport through the column, the second term the dispersive transport and the third term the transport through a film to the particle surface.

$$\frac{\partial c_i}{\partial t} = -u_{int}\frac{\partial c_i}{\partial x} + D_{ax}\frac{\partial^2 c_i}{\partial x^2} - \frac{1-\varepsilon_c}{\varepsilon_c}\cdot\frac{3}{r_p}k_{\mathrm{eff},i}[c_i - c_{p,i}] \quad (2)$$

u_{int} denotes the interstitial velocity, ε_c the column porosity, r_p the particle radius and $k_{\mathrm{eff},i}$ the lumped film diffusion coefficient. D_{ax} displays the axial dispersion, more precisely, a combined effect of dispersion and diffusive processes, dispersion being eddies and all effects implied by three-dimensionality.

The time and position-dependent change of concentration on particle level for the ith component, $\partial c_{p,i}/\partial t$, is analogously described by Eq. (3):

$$\frac{\partial c_{p,i}}{\partial t} = \frac{3}{\varepsilon_p r_p}k_{\mathrm{eff},i}[c_i - c_{p,i}] - \frac{1-\varepsilon_p}{\varepsilon_p}\frac{\partial q_i}{\partial t} \quad (3)$$

with q_i denoting the concentration of particle-bound component i and ε_p the particle porosity, The first term on the right hand side of Eq. (3) displays the mass transfer to particle surface and the second term describes ad- and desorption processes on particle level, i.e. the interaction between mobile and bound phase.

For the description of ad- and desorption processes, the SMA approach was embedded into the mechanistic model. The model equations for n components (n = 1[salt] + number of protein components) are given by

$$\frac{\partial q_i}{\partial t} = k_{ads,i}c_i\overline{q_1}^{\nu_i} - k_{des,i}c_1^{\nu_i}q_i \quad i > 1 \quad (4)$$

$$\Lambda = q_1 + \sum_{i=2}^{n}\nu_i q_i \quad (5)$$

$$\overline{q_1} = q_1 - \sum_{i=2}^{n}\sigma_i q_i \quad (6)$$

Eq. (4) expresses the time dependent change of the concentration of surface bound component i. $k_{ads,i}$ denotes the adsorption rate and $k_{des,i}$ the desorption rate. The parameter Λ (ionic capacity of the adsorbent) limits the available binding places and displays the rivalry between salt concentration q_1 and the other bound components q_i, $2 \le i \le n$ with their specific characteristic charges ν_i. $\overline{q_1}$, the concentration of bound salt ions available for exchange with the protein, is given by the total salt ion concentration q_1 less the shielded ions determined by the protein specific steric factors (σ_i) in Eq. (6). If the assumption of rapid equilibrium is valid ($\partial q_i/\partial t = 0$), Eqs. (4)–(6) can be linked to the SMA isotherm:

$$c_i = \left(\frac{q_i}{k_{eq,i}}\right)\left(\frac{c_1}{\Lambda - \sum_{i=2}^{n}(\nu_i+\sigma_i)q_i}\right)^{\nu_i} \quad i > 1 \quad (7)$$

where the parameter $k_{eq,i}$ is the ratio of ad- and desorption coefficient.

SMA parameters for the mechanistic model can be determined based on data from gradient and breakthrough experiments (compare [34]). The inverse method states a second, equally predictive approach and is directly based on process data and the mechanistic model (see [35]).

3. Materials and methods

3.1. Apparatus, column and software

The case study aims at an optimal separation of a three component mixture on the adsorbent SP Sepharose FF by bilinear gradients. The running buffer in all experiments was 20 mM sodium phosphate buffer at pH 7. The buffer for elution purposes contained additional 0.5 M NaCl. The three component mixture consisted of lysozyme (chicken egg white, L651), ribonuclease A (bovine pankreas, R4875) and cytochrome c (equine heart, C2506) from Sigma (St. Louis, MO, USA) dissolved in the low salt working buffer to a concentration of 0.2×10^{-3} M. Salts and 1 M NaOH for pH adjustment were purchased from Merck (Darmstadt, Germany). The chromatographic setup consisted of a prepacked HiTrap SP Sepharose FF 1 ml column and an Ettan LC system, both purchased from GE Healthcare (Buckinghamshire, United Kingdom). The software MODDE (Umetrics, Umeå, Sweden) was used for DoE and RSM handling. The software Matlab (The Mathworks, Natick, ME, USA) was used for the handling of the mechanistic model.

3.2. Gradient elution experiments

In all experimental setups the column was at first equilibrated with running buffer for 10 column volumes (cv). This step was followed by an automated sample load of 20 μl protein mixture. Then the column was washed for another two cv, before a bilinear elution gradient was initiated. Every elution gradient was applied for exactly 30 cv and quit with 100% high salt elution buffer, followed by a 5 cv high salt wash step. Conductivity and UV-absorbances at 280 nm and 528 nm were measured online at column outlet. Cytochrome c absorbs not only radiation at 280 nm but additionally at 528 nm; this extra information was taken into account when calculating the resolutions between the peaks and for the SMA parameter estimation by the inverse method (see Sections 3.3 and 3.4). The flow rate was set constantly to 0.5 ml/min [ca. 0.22×10^{-3} m/s] in every process step.

The specific shape of a bilinear elution gradient was given by three characteristic factors:

- Initial proportion of elution buffer in the running buffer: **Start** [%].
- Proportion increment of elution buffer in the running buffer at the end of the first part of the bilinear elution gradient: **Slope** [%].

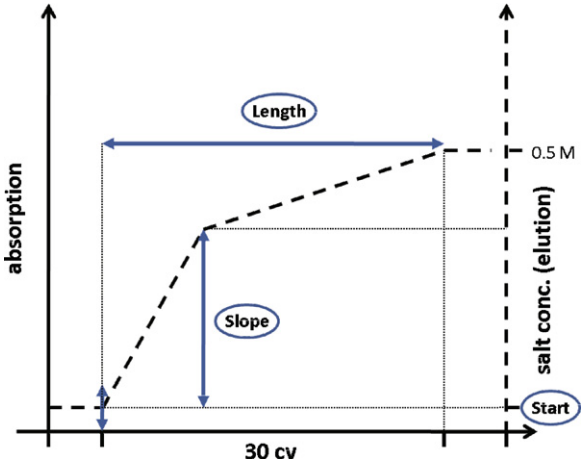

Fig. 1. Three characteristic factors define the shape of the first gradient. The second gradient is determined by the total elution volume (30 cv) and the final salt concentration of 0.5 M NaCl.

- Length of the first gradient of the bilinear elution gradient: **Length** [cv].

while the overall gradient length was set constant to 30 cv and the final salt concentration of the gradient to 0.5 M NaCl. Fig. 1 shows how the shape of a bilinear gradient is defined by the three characteristic factors **Start**, **Length** and **Slope**.

A manipulation of these factors influences the axis intercept, length and slope of the first gradient. For the second part of the gradient these characteristics are implicit, due to the fixed end point of the bilinear gradient at 30 cv and 100% elution buffer (0.5 M NaCl).

Fig. 2 shows a typical chromatogram resulting from an experiment with a bilinear gradient. The preset shape of the gradient is depicted in the dotted line. In all following chromatograms, always the preset gradient shape will be shown and not the measured conductivity, as these measurements did not go into modeling. However, the comparison of the actual conductivity to the results from mechanistical modeling showed excellent consistency. The grey line depicts the absorption signal at 528 nm, which measures the concentration of cytochrome *c*. The black line depicts the absorption signal at 280 nm. The first peak corresponds to the concentration of ribonuclease A and the second peak is the sum signal for the concentrations of cytochrome *c* and lysozyme.

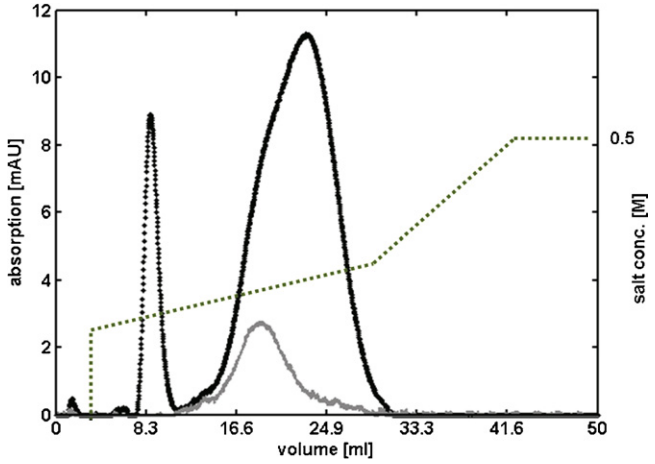

Fig. 2. Typical chromatogram for the separation of ribonuclease A, cytochrome *c* and lysozme with a bilinear gradient. The dotted line shows the settings for the elution gradient. Absorption at 528 nm (cytochrome *c*, grey) and 280 nm (all three proteins, black) is measured online and continuously.

Table 1
Factor ranges for onion design 1.

Factor	Unit	Range
Start	%	20–40
Length	cv	10–20
Slope	%	5–55

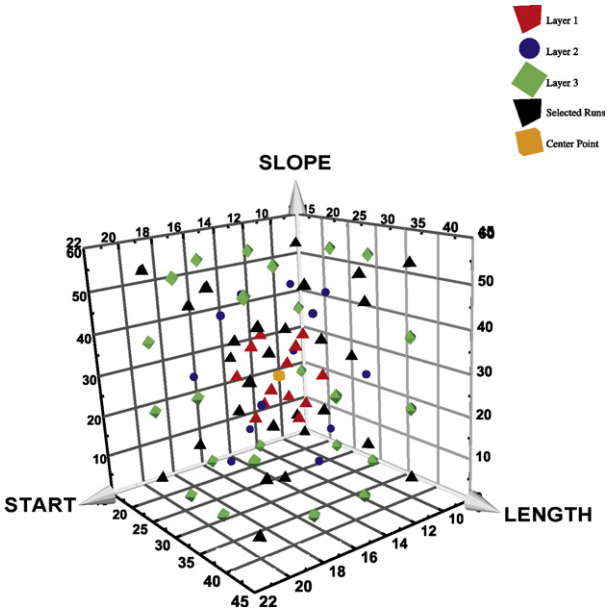

Fig. 3. 3D scatter plot of onion design 1.

3.3. The response surface modeling approach

The experiments were planned based on two D-optimal onion designs. Onion designs are space-filling designs recommended for situations where the factor correlations are not well known. The factor space is divided into layers around a center point, the number of layers and the layer setup is determined by optimality criteria. Onion designs provide information for nonlinear RSM and have the additional advantage of not having to perform experiments at the edges of the factor space (see [36,37] for more details). Although a significant smaller number of experiments would have been possible for a general DoE–RSM approach, a design with 32 measurement points was chosen in this case study. This choice was made in order to prevent a failure of the DoE–RSM-approach due to lack of information. The first design in the presented case study (onion design 1) proposed 29 factor sets in the ranges given in Table 1 and a threefold repetition of a central point for check of reproducibility. The number and distribution of experiments in a layer fulfilled the criteria of G-optimality, minimizing the maximum variance of the predicted values. The distribution of measurements can be seen in Fig. 3. The ranges for the second design that was used in the case study are given in Table 2

A single factor set, consisting of three specific values for **Start**, **Length** and **Slope**, described the unique shape of a bilinear gradient. All experiments, including the three center points, were performed in random order. The center point of onion design 1 was placed in a

Table 2
Factor ranges for onion design 2.

Factor	Unit	Range
Start	%	5–25
Length	cv	15–30
Slope	%	0–15

region, where good separation results were predicted by previous high-throughput screening studies on a robotic platform [8].

The DoE–RSM-approach establishes a functional relationship between the factors **Start**, **Length**, **Slope** on the one hand and the overall peak resolution on the other hand (see Section 2.1). Consequently, the sum of the adjacent peak resolutions was selected to be the objective value that was to be maximized.

The resolutions were calculated along Eq. (8) (compare to [38]):

$$res_{P1,P2} = \frac{2(\mu_{P1} - \mu_{P2})}{4\sigma_{P1} - 4\sigma_{P2}} \tag{8}$$

μ_{P1}, μ_{P2} and σ_{P1}, σ_{P2} are the characteristic first and second central moments, which describe the location and width of a peak. The peaks were deconvoluted based on the additional chromatogram for cytochrome *c* displaying the absorbance at 528 nm.

In Eq. (8) two objectives (small peak width and large distance of retention times) are connected to an objective function. This is a common way to handle multi-objective problems: the objectives are combined and weighted in objective functions that have to be maximized or minimized. Choosing resolution as objective function, both models will optimize the resolution exclusively. In practice, the decision on the objective function is crucial and strongly situation-dependent.

Let f_{RSM} be the empiric model function, a multivariate quadratic function/response surface fitted to the resolution values. All coefficients of f_{RSM} have to be estimated by the inverse method, detecting estimators that induce the best fit of the response surface function to the resolution data. Then, the factor values at the maximum of this function are the characterization of a bilinear gradient that separates the three model proteins best, according to the selected objective, the maximal sum of resolutions.

3.4. The mechanistic model approach

Similar to the coefficients in RSM, the mechanistic model has parameters that have to be determined before model employment. The parameters of mechanistic models for chromatography are characteristic values describing the geometry of the column, the porosities of the packed bed, etc. (compare to Section 2.2). In this study only the sorption parameters for the binding of protein to the adsorbent surface had to be established; all other model parameters had been determined beforehand in [35]. The sorption parameters were determined by the inverse method, shortly explained in the next paragraph.

3.4.1. Determination of SMA parameters

Let $c_{280}(t_j)$ be the time series of protein concentrations monitored by absorption at 280 nm at column outlet at the points in time $j = t_0 \cdots t_{end}$. Let $c_{528}(t_j)$ analogously be the concentration of cytochrome *c* monitored at 528 nm at column outlet. Let $\hat{c}_{280}(t_j, \theta)$ be the solution of the described mechanistic model for chromatography for the sum of all three components concentrations at the same points in time. This solution is dependent from the modeling parameters θ. Let furthermore $\hat{c}_{528}(t_j, \theta)$ be the solution of the same mechanistic model for the component representing cytochrome *c*. Let θ_{fix} be the previously determined set of model input parameters and θ_{est} the set of model input parameters that are estimated based on all available data sets. Here, θ_{est} are the SMA parameters that have to be estimated for all three components, ribonuclease A, cytochrome *c* and lysozyme, based on 62 chromatograms (two 29 point onion designs with triple center points) corresponding to the factor settings $\theta_{grad,k}$ = {Start, Slope, Length}, $1 \le k \le 62$. Aiming at a best fit between model response and chromatographic data, the problem of the inverse method can be stated as an optimization of a sum of least squares:

$$res(\theta_{est}) = \sum_{k=1}^{62} \sum_{j=0}^{end} [(\hat{c}_{280}(t_j, \theta_{fix}, \theta_{grad,k}; \theta_{est}) - c_{280}(t_j))^2 + (\hat{c}_{528}(t_j, \theta_{fix}, \theta_{grad,k}; \theta_{est}) - c_{528}(t_j))^2] \tag{9}$$

minimizing $res(\theta_{est})$. The minimization of Eq. (9) was in all cases performed with the Matlab®-procedure `lsqnonlin`.

3.4.2. Separation optimization

The case study aimed for an optimization of the separation regarding high resolutions between adjacent protein peaks. The resolution between the peaks can be maximized by minimizing the peak overlaps. Let θ_{grad} denote the optimizable parameters, the three factors **Start**, **Length** and **Slope**. For the numerical optimization of the separation process, the unknown parameters $\theta_{optgrad}$ inducing the gradient of least overlap, are the solution of following minimization problem:

$$res_{12}(\theta_{grad}) + res_{23}(\theta_{grad}) + res_{13}(\theta_{grad}) \longrightarrow \min! \tag{10}$$

with

$$res_{k,l} = \sum_{j=t_0}^{t_{end}} (\min(\hat{c}_k(t_j, \theta_{fix}, \theta_{grad}), \hat{c}_l(t_j, \theta_{fix}, \theta_{grad}))) \tag{11}$$

$\hat{c}_i(t_j, \theta)$ being the concentration profile/chromatogram for component *i* calculated by the mechanistic model, θ_{fix} are the mechanistic model parameters that are fixed in the optimization (SMA parameters inclusive).

3.5. Comparison of approaches

The comparison between the described modeling approaches has to be qualitatively as slightly different objective functions have been chosen (compare Eqs. (8) and (10)). This choice has been made in order to keep close to real applications by choosing objective functions corresponding to the typical model response. While the sum of resolutions calculated by Eq. (8) is directly inserted into the DoE–RSM approach for model calibration the mechanistic model is calibrated based on the complete chromatograms that were previously transformed to a time series of concentrations. Thus, the response of the DoE–RSM approach will be a sum of resolutions while the response of the mechanistic model will be a complete noiseless chromatogram with a perfect baseline. To really perform a quantitative comparison with the same objective function on these different model responses, significant data transformations and studies on noise in chromatographic data would have been necessary. This was out of the scope of the manuscript. Although a direct quantitative comparison between the approaches is impossible, the authors are positive, that the shown results allow for a meaningful qualitative comparison and a qualified discussion on advantages and disadvantages.

4. Results

The separation of the three component mixture (ribonuclease A, cytochrome *c* and lysozyme on SP Sepharose FF) was to be optimized. Two approaches, a response surface modeling approach on the one hand and a mechanistic modeling approach on the other hand, were employed for the separation optimization. Both approaches were based on DoE-planned experiments and were to be compared as to their optimizing and predictivity performance.

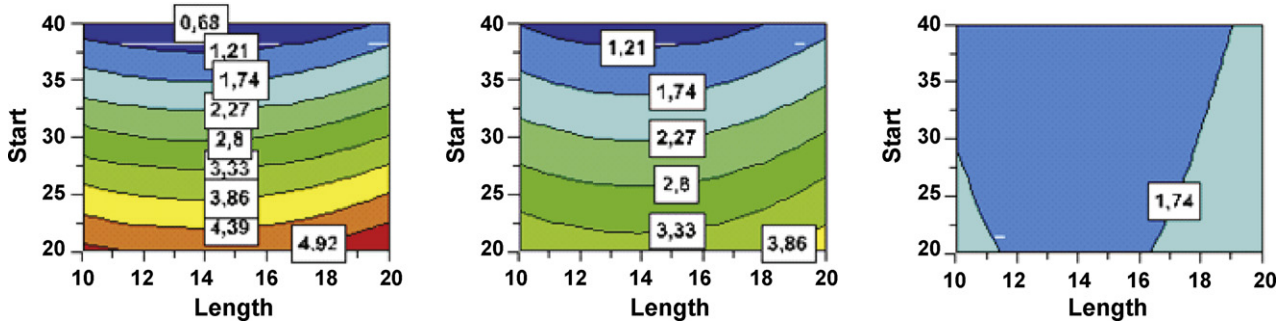

Fig. 4. Surface contour plots based on 31 experiments from onion design 1. The factors **Start** and **Length** span the space, the factor **Slope** is illustrated in three levels: 5 (left-hand subplot), 25 (center), 55 (right-hand). The contour lines show the predicted values for the overall sum of resolutions in the design space.

4.1. Results of the response surface modeling approach

The plot in Fig. 4 is based on the experiments from onion design 1 (see Table 1) and shows the response surface regression of the three explanatory factors (**Start**, **Length** and **Slope**) to the resulting sum of peak resolutions, denoted on the level curves.

The three subplots illustrate three levels of the factor **Slope**. The optimal region of factors in the design space leading to an overall sum of resolution close to 5, is located in the bottom right-hand corner of the left-hand side subplot. Thus, an initial concentration of about 20% salt in elution buffer, a gradient length of the first gradient of 20 cv and a flat slope are predicted to lead to optimal separation results. The supply of predictions over a region that as far as possible surrounds the optimal process conditions is necessary for information on robustness. To keep the approach simple and follow typical procedures, the previously used DoE settings were applied for a second time with slightly shifted and enlarged ranges. Subsequently, the the whole set of 62 results was analysed. The experimental reproducibility *rep* was 0.97, calculated by the variation at the center points compared to the total variation of the responses:

$$rep = 1 - \frac{(1/2)\sum_{i=1}^{3}(cp_i - \overline{cp})^2}{1/(62-1)\sum_{i=1}^{6}2(x_i - \bar{x})^2} \quad (12)$$

where cp_i denote the objective values of the threefold repeated center points, x_i the responses of 62 data points (including the center points) and the bar over a variable implies its mean value. To these data the RSM-method was applied. A quadratic model as initial modeling guess is the most common approach in RSM. In a data-based model discrimination, the model with highest coefficient of determination and with no non-significant paramters (p-value $\leq$ 0.05) was chosen. The best-fitting response surface was a quadratic model function with interaction terms. The regression fit itself had an adjusted coefficient of determination R^2 of about 0.78, what already indicates a limited predictivity.

The coefficient plot in Fig. 5 shows the scaled and centered coefficients for the factors having most effect on the separation result and the factor interactions. The analysis shows that a long first part of the elution gradient induces positive effects on the resolution between the three protein components. This effect increases considerably with rising gradient length, as the coefficient for '**Length***Length' is positive. The factor **Slope** has a slightly positive effect on the resolution of the peaks. Conversely, an increasing salt concentration at gradient begin (factor **Start**), has a negative effect on the overall sum of peak resolutions. These results suggest that gradients with a gentle slope and a low salt concentration at gradient beginning were most successful with respect to the separation problem. In addition, a positive interaction between **Start** and **Slope** with regard to high resolutions is predicted by the model. This interaction effect can be explained by the fact that the combination of both parameters mainly decides on the slope of the first gradient.

The contour plots in Fig. 6 are based on all results from onion design 1 and onion design 2. The three subplots illustrate three levels of the factor **Slope**. The optimal set of factors with respect to a high resolution is located at the right-hand side of the left-hand side subplot. Thus, an initial concentration of about 20% salt in elution buffer and a gradient length of 30 cv together with a very even slope showed the best results. Though placed at the border of the design space, the optimal gradient length of 30 cv could not be further optimized, since the maximum possible gradient length was fixed to 30 cv. The optimal region is very small and the gradient within the contour plot is steep. This indicates a low robustness of the examined system. Small changes in the elution gradient will have significant effects on the separation quality.

Three quantitative RSM-based predictions for the optimal set of factors with respect to a maximal, a medium and a minimal overall sum of resolutions are given in Table 3. RSM predicted a maximal overall resolution for a gradient of 30 cv with constant 10% high salt elution buffer, a medium resolution for the factors listed in the second column and a minimal resolution between the peaks for the factor values in the third column. As these predictions are partly based on a response surface extrapolation, the negative resolution value in the third column of Table 3 is to be regarded as a tendency to a poor resolution.

The experiments with factor settings from Table 3 were performed based on the instructions given in Section 3.2. Fig. 7A shows the experimental results for the factor set in the first column of

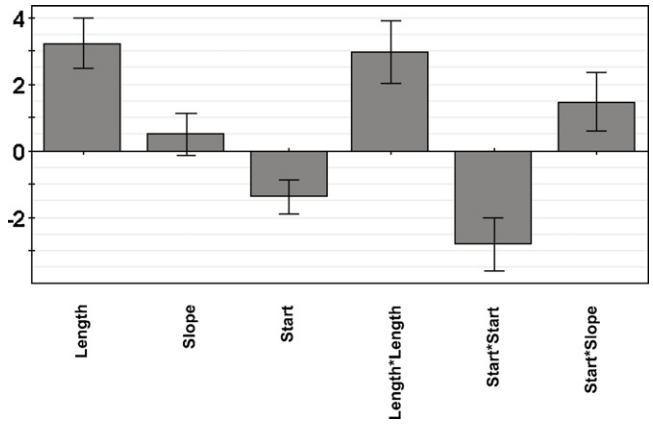

Fig. 5. Coefficient plot for the response surface regression of the three gradient defining factors **Start**, **Length** and **Slope** to the sum of resolutions between the peaks.

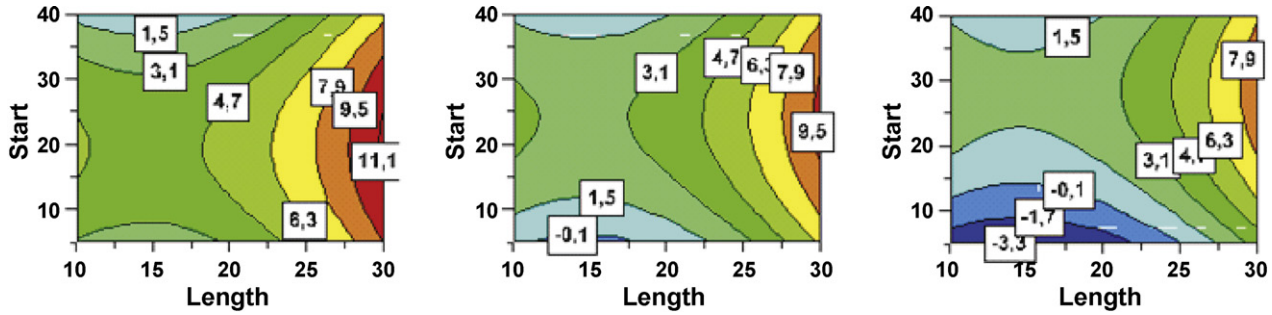

Fig. 6. Surface contour plots based on all 62 experiments. The factors **Start** and **Length** span the space, the factor **Slope** is illustrated in three levels: 0 (left-hand subplot), 27.5 (center), 55 (right-hand). The contour lines show the predicted values for the overall sum of resolutions in the design space.

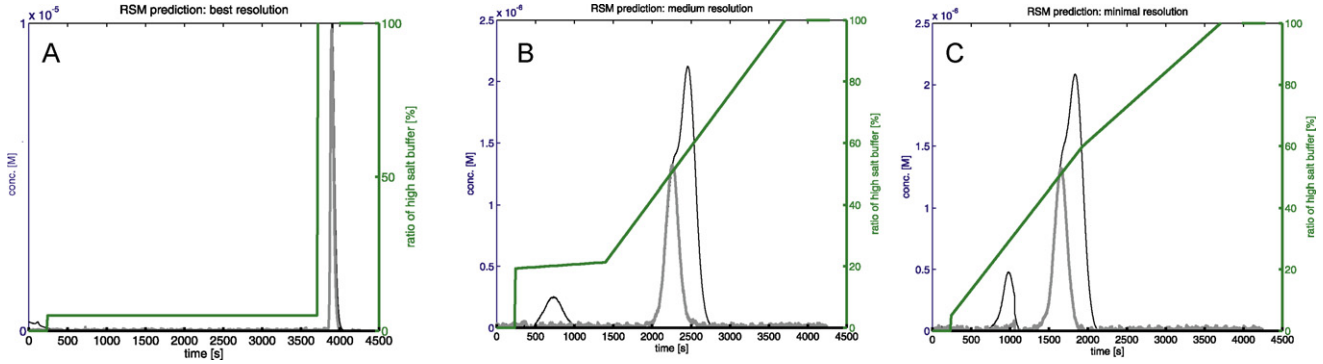

Fig. 7. Experimental results for the RSM-based predictions for a maximal (subfigure A), a medium (subfigure B) and a minimal (subfigure C) resolution in the multicomponent separation of ribonuclease A, cytochrome *c* and lysozyme on SP Sepharose FF (see Table 3). The salt gradient is displayed as ratio of elution buffer. In the chromatograms the black continuous line displays the total protein concentration and the grey line the concentration of cytochrome *c*.

Table 3. Based on the DoE–RSM approach the optimal salt gradient was predicted to be a 30 cv long step at 0.05 M NaCl. The RSM-based prediction failed, as obviously Ribonuclease A, cytochrome *c* and lysozyme elute simultaneously in the high salt wash step, what results in a resolution of 0.1 and not 9.46 (see Table 3) The experimental result for the factors corresponding to the prediction for medium resolution shows in fact a resolution of 4.2, a value, that is close to the predicted resolution of 4.8. (Fig. 7B). The experimental results for the factor set that was predicted to result in a minimal resolution (third column in Table 3) show a sum of resolutions of 2.8 (Fig. 7C). This result has a correct trend, as it is small but obviously it is not minimal.

4.2. Results of the mechanistic modeling approach

The monitored absorbance curves of the experiments planned with two onion designs (see Tables 1 and 2) were employed to determine the SMA parameters by an inverse method. As the steric factor σ had neglegible influence on the fitting result in the ranges of 20–40, it was fixed during the optimization of Eq. (9) to a reasonable value of 30. The estimated SMA parameters for all three components are given in Table 4. These parameters provided the best fit between model response and chromatograms monitored at the Ettan LC system.

The first column shows the estimated characteristic charges for the three proteins, ribonuclease A (1.6), cytochrome *c* (2.8) and lysozyme (3.4). The ascending order of these values correlates with the elution sequence. In addition, adsorption and desorption coefficients were estimated – their ratio can be summed up to the equilibrium coefficient (4th column of Table 4). The parameters in Table 4 are in the limits of experimentally determined SMA parameters and are therefore reasonable (compare for example with parameters in [24,35,39]). The completely calibrated mechanistic model was then employed to predict optimal gradient factors leading to a maximal or minimal sum of resolutions (see Section 3.4.2). The predicted factors for maximal and minimal resolution are presented in Table 5. Particularly the prediction for a minimal overall resolution differs from the RSM-based prediction (see the third column of Table 3).

The optimal gradient, according to the mechanistic model, begins with a concentration of 25.19% of the elution buffer. The slope of the gradient is very smooth. It requires the addition of

Table 3
Predictions for factor sets inducing maximal, medium and minimal overall resolution in the three component system. These predictions are based on the **DoE–RSM**-approach.

Factor	Maximal resolution	Medium resolution	Minimal resolution
Start	10	19.26	40
Length	30	10	26
Slope	0	2.08	55
Predicted resolution	9.46	4.8	−3.3
Exp. determined resolution	0.1	4.2	2.8

Table 4
Table of SMA parameters determined with the inverse method.

	ν	k_{ads}	k_{des}	k_{eq}	σ (fixed)
Ribonuclease A	1.6	6.2	22.16	0.27	30
Cytochrome *c*	2.8	4.6	17.16	0.27	30
Lysozyme	3.4	1.6	11.78	0.14	30

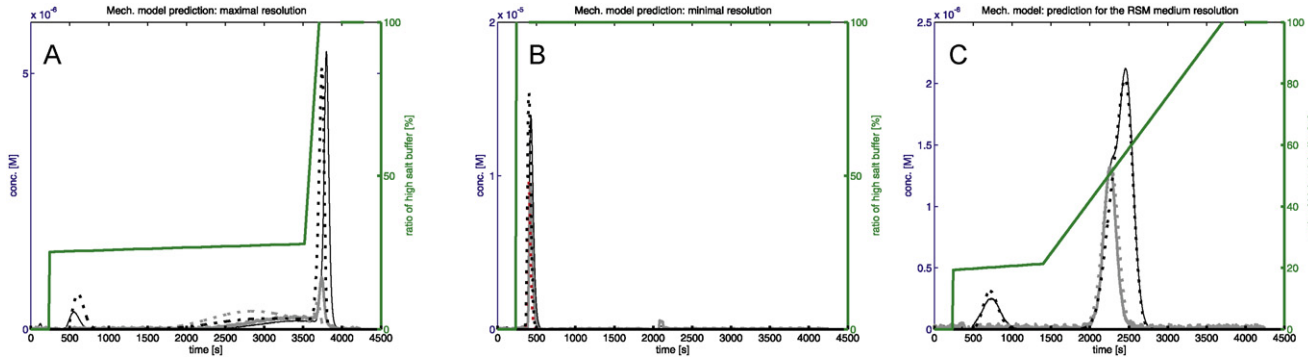

Fig. 8. Results for the mechanistic model-based prediction for a maximal (subfigure A) and minimal resolution (subfigure B) for the separation of ribonuclease A, cytochrome *c* and lysozyme on SP Sepharose FF with a bilinear gradient. The continuous lines display the overall protein concentration (black) and the concentration of cytochrome *c* (grey). The dotted lines display the model-based prediction. Subfigure C shows the chromatogram for the RSM-predicted medium resolution superimposed with the highly accurate model prediction.

0.01% of high salt buffer per cv to the elution buffer. The gradient ends after 28.37 cv with 27.77% of the elution buffer. The mechanistic model proposes, similar to the DoE–RSM-prediction, a step-like gradient for the best resolution between proteins. The corresponding experimental results to the factors given in Table 5 are shown in Fig. 8. The peak predictions for ribonuclease A and lysozyme (first and third peak) are very accurate compared to the experimental data (continuous lines). The prediction for cytochrome *c* (peak in the center) is slightly shifted to reality. Nevertheless, the resolution between all protein peaks is high. The predicted factors for minimal resolution (2nd column of Table 5) induce the chromatogram displayed in Fig. 8B. The resolution is obviously minimal, as salt concentration rises in a step from 0 to 100% and all proteins elute at once. In Fig. 8C again the experimental results for the RSM-predicted medium resolution are shown. In addition, the model response for this gradient is displayed with dotted lines. This figure gives a good example for the high predictivity of the mechanistic model.

Based on these encouraging results, a model-based prediction for a changed objective was employed: the optimization of the specific resolution between only cytochrome *c* and lysozyme.

The optimal separation gradient with respect to the changed objective was predicted with the calibrated mechanistic model and then experimentally validated. Fig. 9 shows the optimized gradient with the predicted chromatogram in dotted lines, whereas experimental data is given in continuous lines. Even though the prediction for cytochrome *c* was again slightly shifted, the favoured resolution between the cytochrome *c* and lysozyme peaks was high, due to this extraordinary gradient with a negative slope at its beginning. Very interesting is the fact that cytochrome *c* elutes in two parts – the major part of it elutes previously to the sharp bend in the gradient and the minor part afterwards. This can be explained by the fact that due to the low salt concentration at the end of the falling gradient, a certain proportion of protein molecules binds again to the column and is only eluted with the following rising salt concentration after the sharp bend in the elution gradient.

Table 5
Predictions for factor sets inducing maximal and minimal overall resolution in the three component system. These predictions are based on **mechanistic modeling**.

Factor	Maximal resolution	Minimal resolution
Start	25.19	100
Length	28.37	30
Slope	2.58	0

5. Discussion

An empiric response surface modeling approach and a mechanistic modeling approach were compared and examined with respect to performance, predictivity and potential synergies considering the optimization of chromatographic separation processes. On the one hand, this comparison and evaluation was performed theoretically (see Section 2), on the other hand a direct comparison of performance was achieved by applying both approaches to a case study: the optimization of bilinear elution gradients for the separation of a three-component mixture. Two of the components had a very similar pI, what increased the problem's complexity.

62 experiments were planned, based on two D-optimal onion designs (see Tables 1 and 2). The high number of experiments was necessary, because the results of the first design (cmp. Fig. 4) showed the optimal settings to lie at the border of the design space.

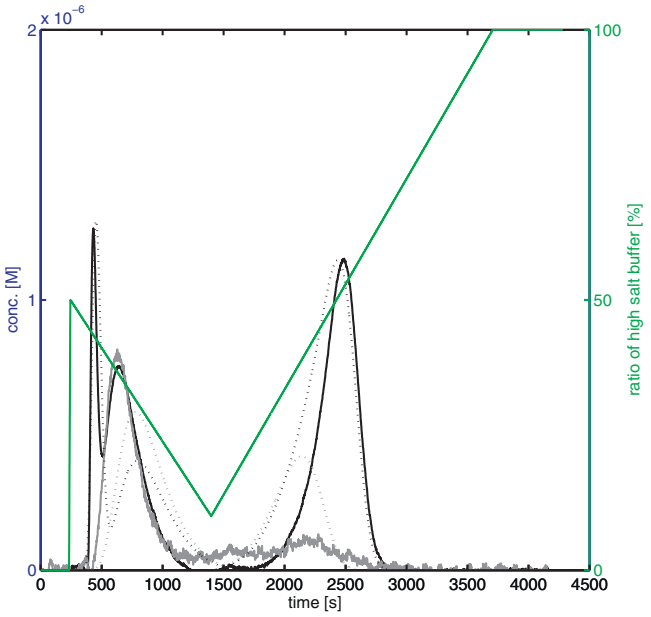

Fig. 9. Result for a model-based optimization of the bilinear gradient considering a maximal resolution between cytochrome *c* and lysozyme. The predicted chromatogram (total protein conc.: black dotted line, cyt. *c* conc.: grey dotted line) and the experimental data (continuous lines) are superimposed.

This situation should be possibly omitted with regard to higher predictiveness of the RSM-model A quadratic model function with interaction terms was fitted to the results of both onion designs. This regression established a functional relationship between the objective function (sum of resolutions) and the gradient shape regulating factors **Start**, **Length** and **Slope**. The coefficient plot (see Fig. 5) revealed the most important factors and their influence on the objective function. Based on this empiric model function and the modeling surfaces (see Fig. 6), the factor setups for different qualities of separation (maximal, medium and minimal resolution) were predicted (see Table 3), the validation experiments were performed and results compared with the predictions (see Fig. 7). The analysis of the response surfaces showed that the examined system is significantly not robust, particularly close to the response surface's maximum. A small change in the shape of the bilinear gradient induces considerable effects on the separation. An example for this are the factors of the optimal gradient predictions of both approaches that are quite close to each other (compare the first columns of Tables 3 and 5); however, the separation results differ significantly (Figs. 7A and 8A). The predictivity analysis of the DoE–RSM-approach showed that the predictions had correct trends but were inaccurate, especially for extremal points. The DoE–RSM-based prediction for the maximal resolution of peaks failed. The same was true for the prediction with respect to a minimal resolution. An important reason for the failure of RSM in the prediction of the separation results, is the fact that the optimal factor set was located at the edge of the design space, where interpolation is more probable to fail due to the lesser number of reference points. The prediction for the minimal resolution probably failed, because extrapolations outside the ranges of the original design space are problematic for empiric RSM, as it only can predict continuous trends. In addition, a very important reason for the low predictivity is indicated by the low coefficient of determination $R^2 = 0.78$. Quadratic RSM can only handle up to quadratic complexity. The lack of fit shows that this system is definitely more complex. As the predictions were based on a model explaining only about 78% of the variety in the experimental data, the probability to fail was increased.

The sorption parameters of the mechanistic model could be determined by the inverse method in this case study based on the DoE-planned datasets (see Table 4). The calibrated chromatography model was employed for the numerical optimization of the separation problem. The elution gradient was optimized with respect to maximal and minimal overall resolution between the component peaks (see Table 5). The validation experiments identified the mechanistic model to be successful and highly predictive (see Fig. 8). The optimal gradients were predicted correctly. While it seems to be obvious for experienced experimenters that an immediate step elution at 0.5 M gives no separation, this fact is not obvious for a model. The correct prediction in this case emphasizes the superiority of the introduced mechanistic modeling approach. The extrapolation of data beyond the borders of the underlying experimental design was possible, because the model is based on mechanistic processes in chromatography.

The prediction of cytochrome *c* data was slightly less accurate than the prediction of retention time and peak shape for the other components. This can be caused by protein–protein-interactions or other effects that were not considered in the modeling, like, for example pH-effects induced by the salt gradient. Without recalibration, an optimal gradient for a high resolution between cytochrome *c* and lysozyme was calculated and the result showed again a high predictivity for extrapolated issues (see Fig. 9). This result could not have been so rapidly achieved with the DoE–RSM approach, as after the recalculation of the specific objective, the multivariate regression function would have needed re-calibration. Moreover, the optimal gradient was again located outside of the original design space, where the RSM-approach has a very low predictivity.

A separation optimization considering different pH conditions was no issue in this manuscript. Definitely a better resolution can be obtained at a different pH condition. Though there are a lot of promising approaches to this modeling issue in mechanistic chromatography models (see [40,41]), no approach is fully established. Thus, a comparison of modeling approaches including the optimization of pH conditions has not yet been made.

5.1. Conclusion and outlook

Two approaches for optimization in chromatography processes, a DoE–RSM approach and an approach based on mechanistic modeling, were to be compared based on their theoretical background and on their performance in a multicomponent separation process.

This comparison revealed advantages and disadvantages of both approaches. An advantage of the DoE–RSM-approach is the comfortable and quick calibration leading to reliable predictions with respect to simple correlations inside the design space. For example, correlations between salt concentration in the buffer at gradient start and the retention time of the first peak could be predicted very accurately (data not shown). Another advantage of the DoE–RSM-approach is the easy identification of factor importance and influences on the objective as well as of the system's robustness.

Nevertheless, the DoE–RSM approach is significantly limited when dealing with complex chromatographic processes. The empiric multilinear model revealed a lack of fit and predictions with respect to an optimal elution gradient for separation failed due to this lack of fit and low robustness of nonlinear gradient elution processes. Results from extrapolation beyond the design space were not reliable as they showed large deviances to the correct results. This fact demands for re-calibration of the DoE–RSM-approach, whenever a new objective is chosen for optimization.

A disadvantage of mechanistic modeling, compared to simple screening methods and the DoE–RSM-approach, is the higher preliminary experimental effort with respect to model calibration and the need for efficient solution algorithms for the partial differential equation system. Nevertheless, it could be shown that the model could easily be calibrated based on the DoE-planned experiments. The predictions inside and beyond the design space were highly accurate and the optimization of the elution gradient was successful for various objectives. Re-calibration was not necessary. The knowledge gain with respect to the process was high, because all parameters are of mechanistic nature. Thus, the completely calibrated model could now be employed for similar separation problems.

The comparison of the two approaches for the optimization of chromatographic separation processes reveals synergies that could lead to new concepts of optimization. Based on these two approaches, an optimization could start with the DoE–RSM-based modeling, revealing factor importances and complexity of the problem. Additionally, this strategy allows for information on robustness issues, for first predictions concerning optimal factor settings and provides sufficient experiments for the calibration of the mechanistic model. The mechanistic model could be calibrated in the next step and be employed for accurate predictions on the process and for the handling of changing objectives as well as for quantitative robustness analysis and process monitoring. This concept will be applied and refined in ongoing research on various (industrial) processes.

Nomenclature

	Unit	Definition
Abbreviation		
cv		column volume
DoE		design of experiments
HTS		high throughput screening
IEC		ion exchange chromatography
RSM		response surface modeling
SMA		steric mass action
c_i	M	concentration of component *i* on column level
$c_{i,p}$	M	concentration of component *i* in the mobile phase on particle level
cp		objective value/response at a DoE-center point
c_{salt}	mM	salt concentration on particle level
D_{ax}	$m^2\ s^{-1}$	axial dispersion
f_{RSM}		empiric response surface model function
$k_{f,i}$	m/s	film transfer coefficient for component *i*
$k_{i,ads}$	$s\,mM^{-\nu}$	adsorption coefficient of component *i*
$k_{i,des}$	$s\,mM^{-\nu}$	desorption coefficient of component *i*
$k_{i,eq}$		equilibrium coefficient of component *i*
L_C	m	column length
n		total number of factors in the experimental plan
q_i	M	concentration of component *i* on the particle surface
R^2		coefficient of determination
r_p	m	particle radius
rep		reproducibility
$res_{P1,P2}$		resolution between peaks belonging to the proteins P1 and P2
u_{int}	ms^{-1}	interstitial flow rate
ε_p		particle porosity
ε_c		column porosity
Λ	M	ionic capacity
μ_P	ml	first moment of the peak belonging to protein P
ν_i		characteristic charge of component *i*
σ_i		steric factor of component *i*
σ_P		square root of the second moment of the peak belonging to protein P
θ_{est}		parameters that will be estimated in the least squares optimization solving the inverse problem
θ_{fix}		parameters that are fixed during the least squares optimization solving the inverse problem
θ_{grad}		parameters/factors that describe the unique shape of a elution gradient

References

[1] D. Fast, P. Culbreth, E. Sampson, Clin. Chem. 28 (3) (1982) 444.
[2] J.C. Berridge, J. Chromatogr. 485 (1989) 3.
[3] V. Drgan, D. Kotnik, M. Novič, Anal. Chim. Acta 705 (1–2) (2011) 315.
[4] J.E. Madden, N. Avdalovic, P.R. Haddad, J. Havel, J. Chromatogr. A 910 (1) (2001) 173.
[5] E. Marengo, E. Robotti, M. Bobba, M.C. Liparota, Curr. Anal. Chem. 2 (14) (2006) 181.
[6] T. Bolanča, Š. Cerjan-Stefanović, M. Luša, Š. Ukić, M. Rogošić, Sep. Sci. Technol. 45 (2) (2010) 236.
[7] K. Kaczmarski, D. Antos, Acta Chromatogr. 17 (2006) 20.
[8] A. Susanto, K. Treier, E. Knieps-Grünhagen, E. Von Lieres, J. Hubbuch, Chem. Eng. Technol. 32 (2009) 140.
[9] M. Max-Hansen, F. Ojala, D. Kifle, N. Borg, B. Nilsson, J. Chromatogr. A 1218 (51) (2011) 9155.
[10] F.D.A.U.S. Department of Health and Human Services (Ed.), Guidence for Industry PAT – A Framework for Innovative Pharmaceutical Manufacturing and Quality Assurance, 2004.
[11] L. Pullan, J. Liq. Chromatogr. Relat. Technol. 11 (13) (1988) 2697.
[12] W. Bachman, J. Stewart, J. Chromatogr. 481 (21) (1989) 121.
[13] M.H.J. Bergqvist, P. Kaufmann, Lipids 28 (7) (1993) 667.
[14] A. Nguyen, T. Aerts, D. Van Dam, P. De Deyn, J. Chromatogr. B 878 (2010) 3003.
[15] S.L.C. Ferreira, R.E. Bruns, E.G.P.d. Silva, W.N.L. Dos Santos, C.M. Quintella, J.M. David, J.B.d. Andrade, M.C. Breitkreitz, I.C.S.F. Jardim, B.B. Neto, J. Chromatogr. A 1158 (1–2) (2007) 2.
[16] D. Bylund, A. Bergens, S. Jacobsson, Chromatographia 44 (1–2) (1997) 74.
[17] P. Lebrun, B. Govaerts, B. Debrus, A. Ceccato, G. Caliaro, P. Hubert, B. Boulanger, Chemom. Intell. Lab. Syst. 91 (1) (2008) 4.
[18] G. Guiochon, J. Chromatogr. A 965 (1–2) (2002) 129.
[19] B. Nfor, P. Verhaert, L. van der Wielen, J. Hubbuch, M. Ottens, Trends Biotechnol. 27 (12) (2009) 673.
[20] P. Jandera, J. Churáček, J. Chromatogr. 91 (1974) 223.
[21] J. Ståhlberg, J. Chromatogr. A 855 (1) (1999) 3.
[22] J. Mollerup, Chem. Eng. Technol. 31 (6) (2008) 864.
[23] S. Gallant, A. Kundu, S. Cramer, Biotechnol. Bioeng. 47 (3) (1995) 125.
[24] S. Gallant, S. Vunnum, S. Cramer, J. Chromatogr. A 725 (2) (1996) 295.
[25] V. Natarajan, B. Bequette, S. Cramer, J. Chromatogr. A 876 (1–2) (2000) 51.
[26] N. Jakobsson, M. Degerman, E. Stenborg, B. Nilsson, J. Chromatogr. A 1138 (1–2) (2007) 109.
[27] H. Kempe, A. Axelsson, B. Nilsson, G. Zacchi, J. Chromatogr. A 846 (1–2) (1999) 1.
[28] E. von Lieres, J. Andersson, Comput. Chem. Eng. 34 (8) (2005) 1180.
[29] C. Brooks, S. Cramer, AIChE J. 38 (1992) 1969.
[30] N. Titchener-Hooker, S. Chan, D.G. Bracewell, AIChE J. 54 (4) (2008) 965.
[31] L. Pedersen, J. Mollerup, E. Hansen, A. Jungbauer, J. Chromatogr. B 790 (1–2) (2003) 161.
[32] S.D. Gadam, G. Jayaraman, S.M. Cramer, J. Chromatogr. A 630 (1–2) (1993) 37.
[33] P. Danckwerts, Chem. Eng. Sci. 2 (1) (1953) 1.
[34] A.A. Shukla, S.S. Bae, J.A. Moore, K.A. Barnthouse, S.M. Cramer, Ind. Eng. Chem. Res. 37 (1010) (1998) 4090.
[35] A. Osberghaus, S. Hepbildikler, S. Nath, M. Haindl, E. von Lieres, J. Hubbuch, J. Chromatogr. A 1233 (2012) 54, doi:10.1016/j.chroma.2012.02.004.
[36] I.-M. Olsson, J. Gottfries, S. Wold, Chemom. Intell. Lab. Syst. 73 (1) (2004) 37.
[37] I.-M. Olsson, J. Gottfries, S. Wold, J. Chemom. 18 (12) (2004) 548.
[38] H. Vink, J. Chromatogr. 69 (1972) 237.
[39] A. Ladiwala, K. Rege, C.M. Breneman, S.M. Cramer, J.M. Prausnitz, Proc. Natl. Acad. Sci. U. S. A. 102 (33) (2005) 11710.
[40] J.C. Bosma, J.A. Wesselingh, AIChE J. 44 (11) (1998) 2399.
[41] T. Yang, M.C. Sundling, A.S. Freed, C.M. Breneman, S.M. Cramer, Anal. Chem. 79 (23) (2007) 8927.